

The macroscopic symmetry of  $\text{Pb}(\text{Mg}_{1/3}\text{Nb}_{2/3})_{1-x}\text{Ti}_x\text{O}_3$  in the morphotropic phase boundary region ( $x = 0.25\text{--}0.5$ )

This article has been downloaded from IOPscience. Please scroll down to see the full text article.

2005 J. Phys.: Condens. Matter 17 5709

(<http://iopscience.iop.org/0953-8984/17/37/009>)

View [the table of contents for this issue](#), or go to the [journal homepage](#) for more

Download details:

IP Address: 129.252.86.83

The article was downloaded on 28/05/2010 at 05:57

Please note that [terms and conditions apply](#).

# The macroscopic symmetry of $\text{Pb}(\text{Mg}_{1/3}\text{Nb}_{2/3})_{1-x}\text{Ti}_x\text{O}_3$ in the morphotropic phase boundary region ( $x = 0.25\text{--}0.5$ )

V A Shuvaeva, A M Glazer and D Zekria

Physics Department, Clarendon Laboratory, University of Oxford, Parks Road, Oxford OX1 3PU, UK

Received 12 May 2005, in final form 8 August 2005

Published 2 September 2005

Online at [stacks.iop.org/JPhysCM/17/5709](http://stacks.iop.org/JPhysCM/17/5709)

## Abstract

The macroscopic symmetry of  $\text{Pb}(\text{Mg}_{1/3}\text{Nb}_{2/3})_{1-x}\text{Ti}_x\text{O}_3$  (PMN–PT) crystals with  $x = 0.25\text{--}0.5$  has been studied by optical microscopy. Precise data on the temperature dependence of the birefringence and optical extinction directions have been obtained. Two different low-symmetry phases separating rhombohedral and tetragonal phases have been observed in the compositional range  $x = 0.3\text{--}0.47$ . The optical extinction in the range  $x = 0.3\text{--}0.37$  is consistent with  $Cm$  space group symmetry, while for  $x = 0.37\text{--}0.47$   $Pm$  symmetry is appropriate. Gradual rotation of the optical indicatrix has been found at temperatures just below  $T_c$  in crystals with  $x = 0.27\text{--}0.3$ . A refined phase diagram is presented.

## 1. Introduction

The compositional changes in the  $\text{Pb}(\text{Mg}_{1/3}\text{Nb}_{2/3})_{1-x}\text{Ti}_x\text{O}_3$  (PMN–PT) system result in the transformation of macroscopic symmetry from tetragonal symmetry in pure  $\text{PbTiO}_3$  to rhombohedral symmetry observed on the PMN-rich side [1]. A similar symmetry transformation takes place in  $\text{PbZr}_{1-x}\text{Ti}_x\text{O}_3$  [2]. The mechanisms of these temperature and compositional transformations have long been a subject of intensive discussions, since there is no group–subgroup relationship between tetragonal and rhombohedral symmetries [3–5]. For a long time it was believed that the tetragonal and rhombohedral phases had a sharp boundary between them (the so-called morphotropic phase boundary, MPB) at about  $x = 0.35$ , and according to the early phase diagrams the phase transition with temperature between these two phases occurred in the range  $x = 0.3\text{--}0.35$  [1, 6–8].

The MPB region has always been the subject of special interest because of the advanced piezoelectric performance and high dielectric permittivity displayed by the material in this compositional range [9–12], which is important for a broad range of applications. The connection between the properties and the macroscopic symmetry can provide useful insight into developing a comprehensive theory and understanding of the origin of the properties.

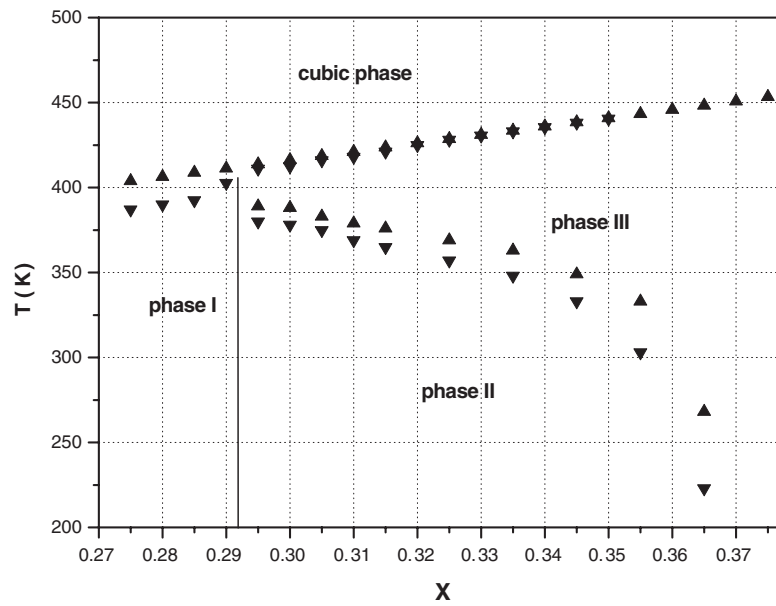


**Figure 1.** The phase diagram of PMN–PT in the MPB region measured on heating and on cooling [17].

Progress in understanding the process of symmetry transformation in PMN–PT has recently been achieved through the discovery of a new phase intermediate between the tetragonal and rhombohedral phases in the range  $x = 0.3–0.36$  [13–15]. The symmetry of this phase was determined to be monoclinic, based on diffraction patterns obtained from powder samples. Low-symmetry distortions have also been seen in optical studies [16]. The boundaries of the intermediate phase have been determined using x-ray diffraction [15], and these were later refined to high precision through optical measurements [17]. The resulting phase diagram is presented in figure 1. The monoclinic phase is labelled phase II in the diagram. The symmetry of phase I is rhombohedral according to the majority of the studies, while phase III was generally believed till now to be tetragonal.

However, the question about the symmetry of PMN–PT in the MPB region and its connection with its properties is far from clear. Controversy persists about the monoclinic phase as to whether it should be described in space group  $Cm$  or  $Pm$  [13, 15, 18]. In addition, accurate analysis of diffraction patterns has provided evidence for two different monoclinic phases, with symmetry  $Cm$  and  $Pm$ , in the range  $x = 0.27–0.34$  [19]. However, in many recent optical studies the symmetry of phase II is still reported to be rhombohedral [20–22], although low-symmetry distortions have been observed at temperatures above the phase transition from phase II to phase III [20–24], which suggest that the crystal system of phase III may not be tetragonal after all. A change of slope in  $T_c$  with composition, which has been reported recently [17] to occur at about  $x = 0.47$ , is also an indication that there may be another hereto unreported phase boundary at about this composition.

This shows a necessity for a more careful consideration of the symmetry of each phase over a wider compositional range across the MPB region. In this paper we address this question by applying optical polarizing microscopy including birefringence imaging using the Metripol rotating polarizer system [25].

## 2. Experimental details

### 2.1. Samples

A number of PMN–PT samples of different compositions with  $x$  varying from 0.25 to 0.5 were used in these studies. Most of them were made by flux growth from a stoichiometric mix of nominal composition prepared from PbO, MgO, Nb<sub>2</sub>O<sub>5</sub> and TiO<sub>2</sub>, plus a 300% mass excess of PbO to serve as the flux, thereby avoiding any other chemicals which may introduce extrinsic impurities. Details of the growth were described elsewhere [17]. We also employed crystals kindly provided by iBULe Photonics Co., Ltd (Korea) (<http://www.ibule.com/eng/pr.html>) grown by the Bridgman method.

Since crystals with well formed (100)<sup>Note 1</sup> natural faces were available, these were selected to serve as convenient references for polishing the crystal sections in corresponding orientations. Some well formed cube-shaped single crystals up to 8 mm were selected, and then polished parallel to the pseudocubic (100) plane down to a thickness of approximately 50  $\mu\text{m}$ , using 1  $\mu\text{m}$  diamond paste.

The compositions of the samples were determined by electron-probe microanalysis (EPMA) (Jeol JXA-8600). This technique allowed the local composition at any position on the surface of the sample to be measured. Corresponding locations were studied with EPMA and optically, so that the correct association between composition and phase transition temperature could be made even when the crystal was inhomogeneous. A spot size of about 10  $\mu\text{m}$  was used. Some of the flux-grown crystals showed a significant composition gradient which enabled us to study the symmetry transformations in the MPB region for a number of different compositions from just one crystal.

### 2.2. Optical microscopy and crystal symmetry

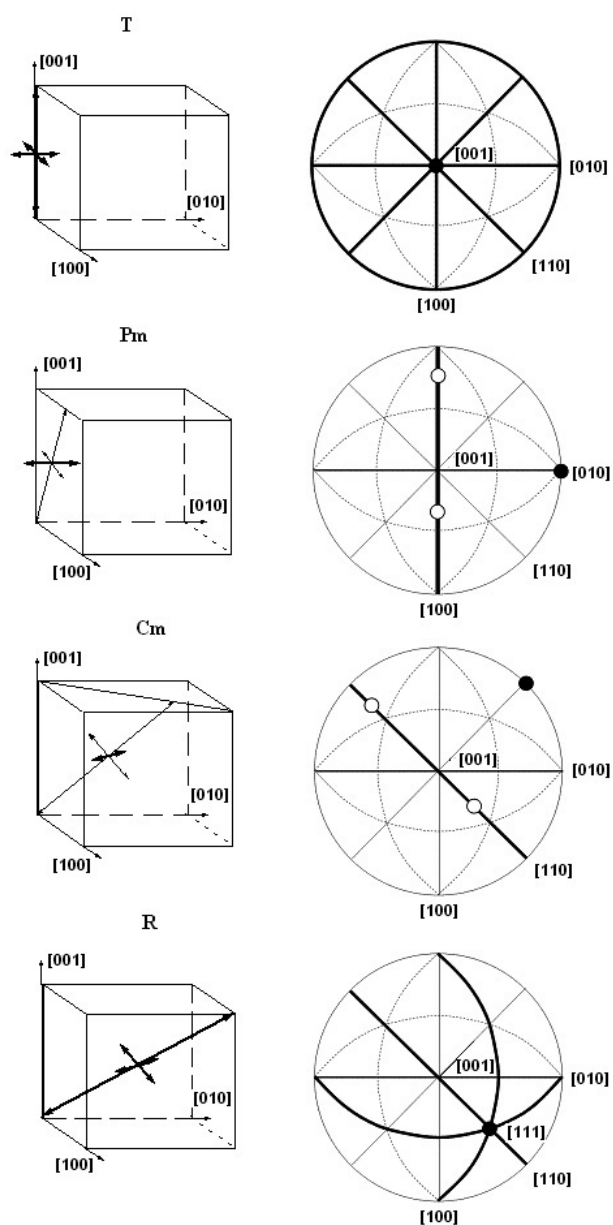
The high sensitivity of the orientation of the optical indicatrix with respect to the macroscopic symmetry makes optical microscopy a very sensitive instrument for studying the symmetry of crystals.

In figure 2 we show the possible optical indicatrix orientations for pseudocubic perovskites allowed for different symmetries, such as rhombohedral, tetragonal, monoclinic  $Pm$  and monoclinic  $Cm$ . In rhombohedral  $R$  ( $R3m$ ) and tetragonal  $T$  ( $P4mm$ ) symmetries the main optic axis of the indicatrix is aligned along the [111] and [001] directions, respectively. In the monoclinic  $M$  phases one of the indicatrix axes is constrained to be *perpendicular* to the mirror plane with the other two perpendicular axes free to lie anywhere *within* the mirror plane. We can distinguish two cases:  $Pm$ , in which the constrained axis is along [010] and  $Cm$ , in which it lies along  $[\bar{1}10]$  (according to the notation of Vanderbilt and Cohen [4] these are phases  $M_C$  and  $M_A$  ( $M_B$ ) respectively).

In table 1 we show the observable optical extinction directions with respect to the [100], [010] and [001] pseudocubic axes for tetragonal, rhombohedral and the two types of monoclinic symmetries.

In the tetragonal phase total extinction is observed on looking down the [001] direction. On viewing down [100] and [010] parallel extinction is observed. In the rhombohedral phase all three projections of the optic axis form an angle of 45° with the pseudocubic main axes (so-called symmetric extinction). In the monoclinic phases the extinction may be different from 45° or 90°, showing oblique extinction, which is evidence of low symmetry. The  $Cm$  monoclinic phase displays symmetric extinction when viewed down [001], whereas in the  $Pm$  phase parallel extinction should be observed.

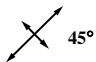
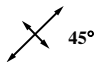
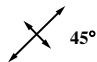
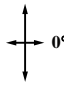
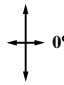
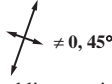
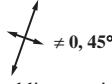
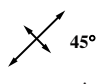
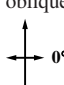
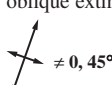
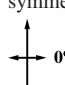
<sup>1</sup> In this paper all references to crystallographic planes and directions are to the perovskite pseudocubic axes.



**Figure 2.** The optical indicatrix orientations relative to the pseudocubic perovskite cell in tetragonal, rhombohedral and two monoclinic phases and corresponding stereographic projections. Indicatrix axes whose direction is fixed by symmetry are shown in bold arrows and black circles correspondingly, while indicatrix axes that lie anywhere within a mirror plane are shown in thin arrows and white circles.

Thus we can see that the set of possible orientations is unique for each type of symmetry. Since the PMN–PT crystals are always twinned we can expect to observe all the possible orientations of the optic axis projections just from one crystal slice with a face parallel to one of the main pseudocubic directions, making it possible to distinguish all the phases listed above using optical microscopy.

**Table 1.** Extinction directions as seen down the three pseudocubic axes (the principal perovskite directions are vertical and horizontal).

Viewing direction	[100]	[010]	[001]
<b>R</b>	 symmetric extinction	 symmetric extinction	 symmetric extinction
<b>T</b>	 parallel extinction	 parallel extinction	Total extinction
<b>M<sub>A</sub> or M<sub>B</sub> = Cm</b>	 oblique extinction	 oblique extinction	 symmetric extinction
<b>M<sub>C</sub> = Pm</b>	 parallel extinction	 oblique extinction	 parallel extinction

Twinned crystals may contain several layers of domains with different orientations of the optical indicatrix. In the R and T phases such twinning will affect only the absolute value of the birefringence, since the possible angles between the projections of the optical indicatrix axes are  $0^\circ$  or  $90^\circ$ . In the monoclinic phases the crystal may not show extinction at all since the angle between projections of the optical indicatrix axes in the twins may have any value. The absence of extinction of a crystal under crossed polarizers is another indication of low-symmetry distortions.

### 2.3. Metripol optical measurements

Along with a conventional polarizing microscope we also used a computer-controlled optical system, Metripol [25], based on a rotating-polarizer method. The elements of this system are an optical polarizing microscope equipped with a computer-controlled rotating polarizer, a CCD camera and software for image capture and analysis. The technique provides false-colour images of the distribution of  $|\sin \delta| = |\sin(\Delta n L 2\pi/\lambda)|$  ( $\Delta n$ —planobirefringence,  $L$ —crystal thickness,  $\lambda$ —light wavelength) and the extinction directions  $\varphi$  ( $\varphi$  is assigned normally to be the slow polarization orientation (*axis*) in regions where  $2n\pi < \delta < (2n + 1)\pi$ , while it is assigned to the fast axis where  $(2n - 1)\pi < \delta < 2n\pi$ ). Thus the method provides a means for accurate numerical analysis of the data.

All the measurements were made at a wavelength of 600 nm. Thermal changes were studied by means of a Linkam TP93 heating stage. The temperature was changed at a rate of  $1 \text{ K min}^{-1}$  while the images were captured with 0.5 K steps. Data extracted from the images were used to make plots of the temperature variation of  $|\sin \delta|$  and  $\varphi$  at several selected points in the crystals. This technique allowed us to obtain average values or to plot diagrams of their distribution over any selected area.

## 3. Results and discussion

As has already been shown in a previous paper [17] three different phases can be clearly distinguished within the composition range  $0.28 < x < 0.38$  through the contrast in their

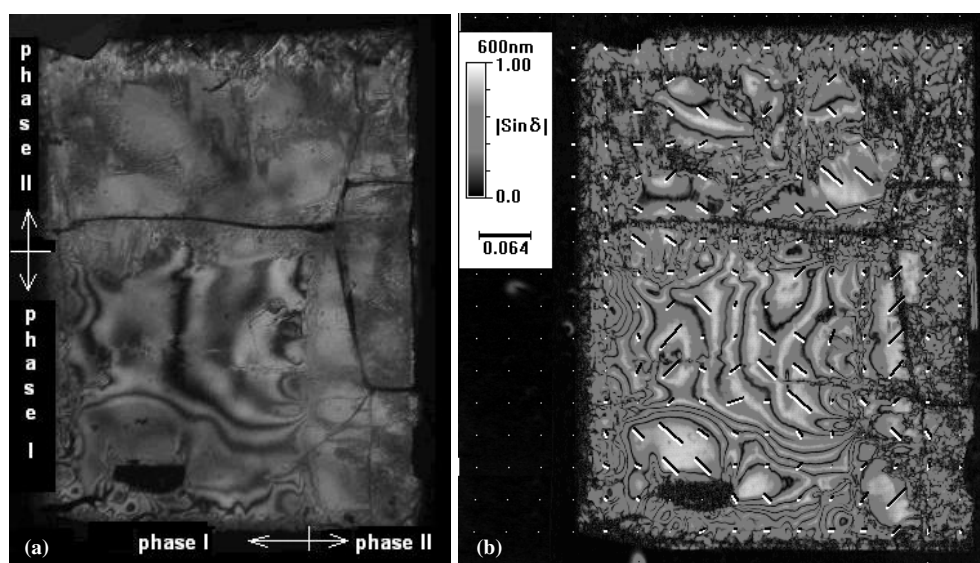


**Figure 3.** PMN–PT crystal with  $x$  varying from 0.26 to 0.35 (a) between crossed polarizers, (b) Metripol  $|\sin \delta|$  image (dashes show one of the extinction directions). The principal perovskite directions are vertical and horizontal. The horizontal scale bar is equal to 0.064 mm. A clear boundary is seen between phase I (bottom left corner) and phase II (the rest of the crystal).

birefringence and difference of domain structure. The contrast is clearly seen in figure 3 showing a PMN–PT crystal with  $x$  varying from 0.26 to 0.35, placed between crossed polarizers, and a corresponding Metripol image. Phase I (bottom left corner) and phase II (the rest of the sample) coexist in this crystal, because of the varying composition. Thin stripes of phase III can be also observed at the crystal edges.

In phase I the birefringence is very low and inhomogeneous, so that in some parts of the crystal it even reaches a value close to zero. No clear domain boundaries can be observed. In contrast, phase II has a high birefringence and a distinct domain structure. At the boundary between these two phases a jump in thermal hysteresis of  $T_c$  is observed.

The phase transition from phase II into phase III, which occurs at temperatures ranging from 200 to 390 K, depending upon the composition, results in an abrupt reduction of birefringence and a step-like change of extinction angle.

Below we present results on the extinction directions and their change with temperature in each of the phases. The smooth one-dimensional compositional gradient in our samples enabled us to observe clearly all the steps of the complex series of phase transformations simultaneously with respect to composition and temperature.

### 3.1. Phases I and I'

In figure 4 the  $|\sin \delta|$  and  $\varphi$  Metripol images of a crystal with a horizontal gradient of composition  $x$  varying from 0.27 to 0.31 are shown for different temperatures. The  $|\sin \delta|$  value is shown through the variation of a grey scale, and one of the extinction directions is marked by dashes. In this crystal the cubic phase boundary moves gradually with temperature in a horizontal direction. As has been shown already [17], the jump in hysteresis of  $T_c$  occurs at  $x = 0.295$ , suggesting that this composition may mark the boundary between two

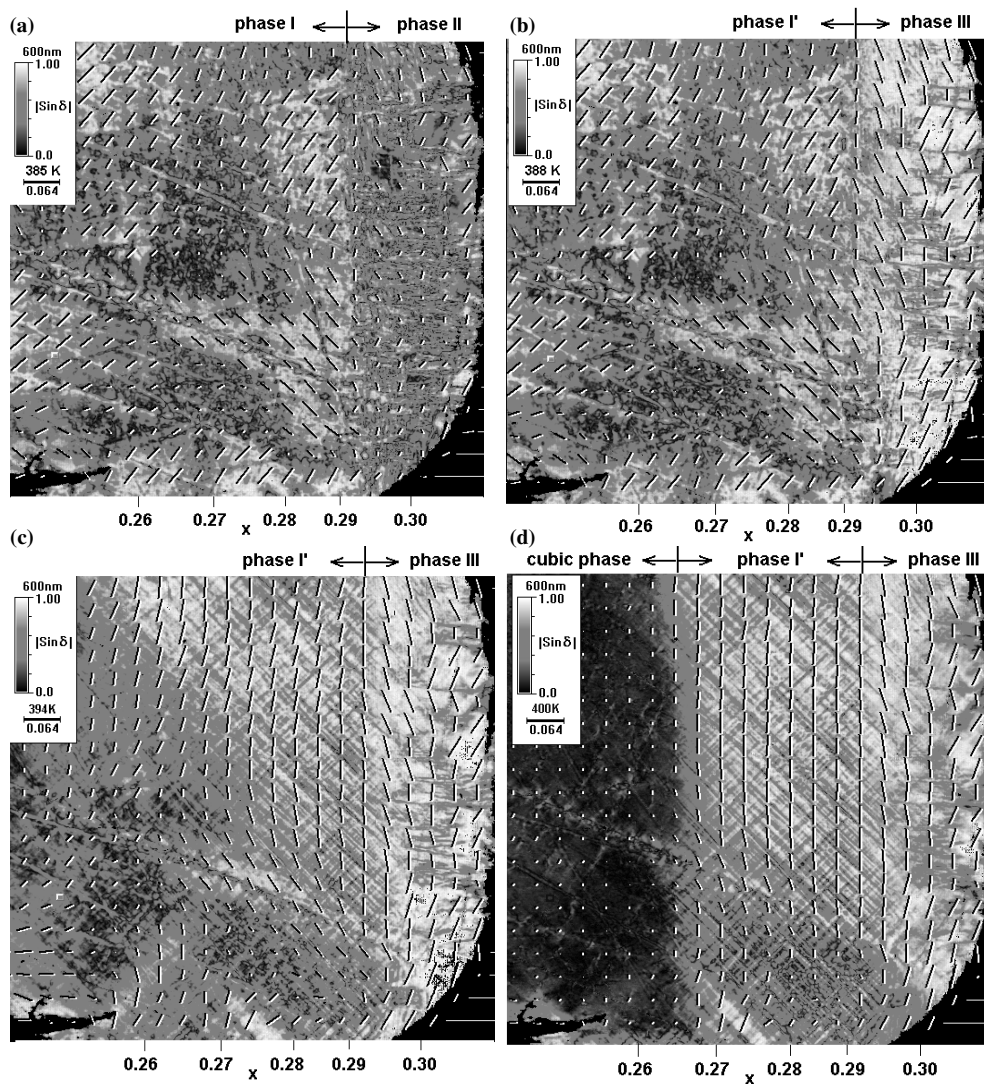


**Figure 4.** The development of birefringence (grey scale) and extinction angle  $\varphi$  with temperature in PMN–PT with a horizontal compositional gradient  $x = 0.25\text{--}0.31$ . The principal perovskite directions are vertical and horizontal. The horizontal scale bar is equal to 0.064 mm. (a)  $T = 385$  K, (b)  $T = 388$  K, (c)  $T = 394$  K, (d)  $T = 400$  K.

different phases. According to dielectric measurements [26, 27] the same composition marks the boundary between relaxor and non-relaxor states. A clear boundary between phase I and phases II and III can be seen at this composition in the Metripol images at all temperatures, indicated by changes of both  $|\sin \delta|$  and  $\varphi$ .

Although monoclinic distortions for  $x < 0.3$  were reported by Singh *et al* [19], according to most studies, phase I is rhombohedral. In all our samples with  $x < 0.295$  at temperatures up to 285 K symmetric extinction occurred with a very small gradual variation of extinction angle over different parts of the crystal. In all the crystals the extinction formed an angle  $\varphi$  close to  $45^\circ$  with the [100] direction, which is consistent with rhombohedral symmetry.



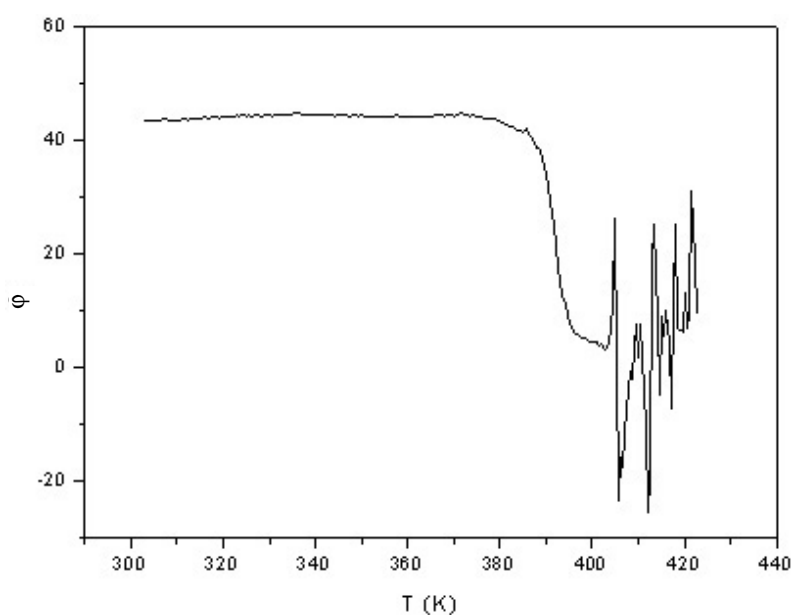


**Figure 5.** The temperature dependence of the optical extinction direction seen on (100) measured from the [100] direction in  $\text{Pb}(\text{Mg}_{1/3}\text{Nb}_{2/3})_{0.72}\text{Ti}_{0.28}\text{O}_3$ .

However at higher temperatures a gradual rotation of  $\varphi$  was observed. The temperature dependence of  $\varphi$  for  $x = 0.28$  is shown in figure 5. It can be seen that  $\varphi$  changes continuously but quite rapidly in the temperature range 385–395 K approaching  $0^\circ$ , so that at high temperatures the observed extinction is consistent rather with tetragonal symmetry. At the same time, the appearance of a quite clear domain structure is observed. This transformation occurs at the same temperatures as the phase transition from phase II to phase III for  $x > 0.295$ , and may indicate a phase transition from phase I to a new phase, which we shall denote  $I'$ . This phase transition has also been seen using diffraction techniques by Bai *et al* [28], who reported a tetragonal phase in a narrow compositional range between the rhombohedral and cubic phases. At the present time we cannot be sure about the symmetry of phase  $I'$ , although the optical extinction is consistent with tetragonal symmetry.

The differences in birefringence,  $\varphi$  and domain structure indicate that phases  $I'$  and III are different from each other. The boundary between them is also marked by a jump in the hysteresis of  $T_c$ . The phase transition from phase II to phase III results in a jump in birefringence, while the phase transition from phase I to phase  $I'$  occurs with no observable boundary, although a gradual reduction of birefringence can be observed. In figure 4(c) phase  $I'$  appears for  $x < 0.295$  and phase III for  $x > 0.295$ .

A further transformation to the cubic phase occurs at 405 K. In figure 5 random variations of  $\varphi$  are observed at high temperatures corresponding to the cubic phase: this occurs because the cubic phase displays total extinction and this means that  $\varphi$  is not defined in this region.

### 3.2. Phase II

Controversy about the symmetry of phase II persists, although it has been intensively studied by optical microscopy and diffraction techniques [14–23]. It was believed that the structure in

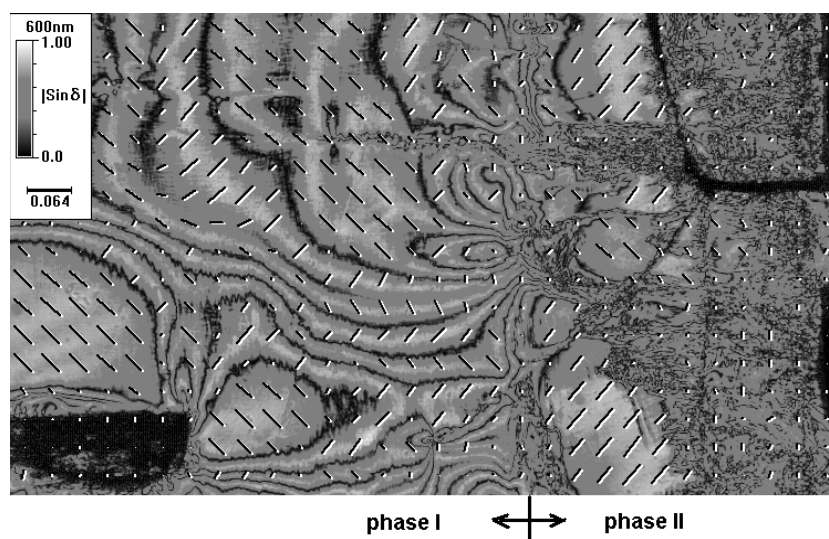


**Figure 6.** Metripol  $|\sin \delta|$  image of a PMN–PT crystal with  $x$  varying from 0.26 to 0.35 (dashes show one of the extinction directions). The principal perovskite directions are vertical or horizontal. The horizontal scale bar is equal to 0.064 mm.

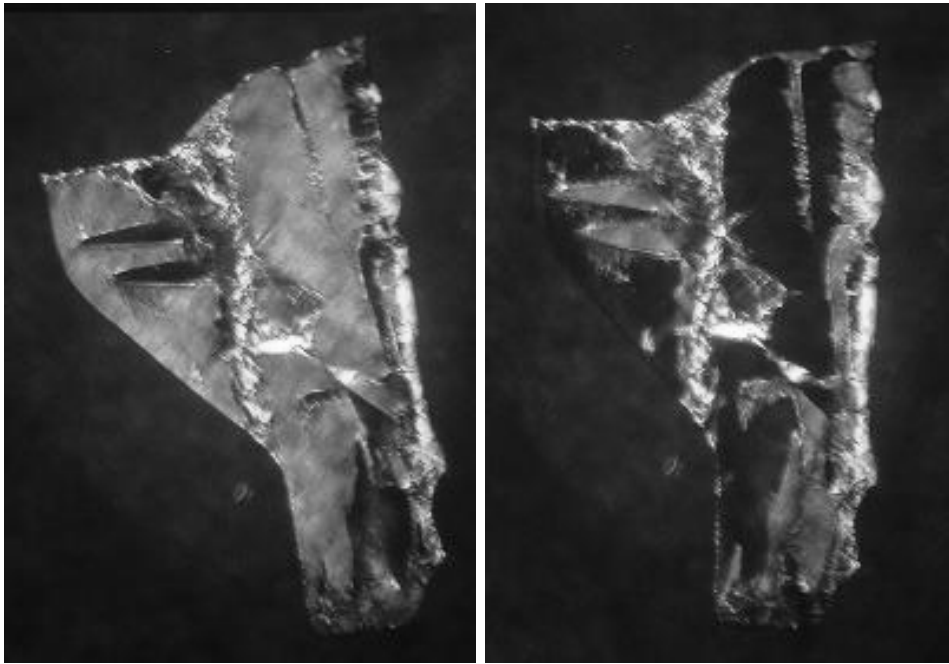
this composition region was rhombohedral until the latest experimental results indicated the presence of monoclinic distortions [13–16]. However there is still no general agreement on whether the phase is rhombohedral, monoclinic  $Cm$  or monoclinic  $Pm$ .

Figure 6 shows a Metripol image of the lower part of the sample, shown in figure 3. Because of the composition gradient the crystal contains both phase I (left-hand side) and phase II (right-hand side). It can be seen that in phase II the deviation of the extinction direction from [111] is quite small and hardly noticeable, which makes it rather difficult to reveal any low-symmetry distortions by optical methods. It is therefore unsurprising that the true symmetry of this phase was not recognized for a long time. Recent optic studies of this phase [22] showed that total extinction can be achieved at room temperature in an electrically polarized (111)-cut single crystal  $\text{Pb}(\text{Mg}_{1/3}\text{Nb}_{2/3})_{0.67}\text{Ti}_{0.33}\text{O}_3$ , leading to the conclusion that the phase is rhombohedral.

In spite of the fact that the extinction in the phase is very close to that which would be expected for a rhombohedral phase, in twinned samples two types of domains showing extinction at different angles can be clearly seen, which is evidence of lower-symmetry distortions. One such crystal, seen between crossed polarizers, is shown in figure 7. The angle between the two crystal orientations at which different domains display extinction is about  $6^\circ$ .

Although we studied a number of crystals within the monoclinic phase region II we did not find any domains with a deviation of the extinction direction of more than  $6^\circ$  from that expected in a rhombohedral crystal. Since we never find parallel extinction in this phase we can conclude that our optical data are consistent with  $Cm$  monoclinic symmetry.

At higher temperatures phase II transforms into phase III as a result of a first-order phase transition, which is accompanied by a step-like change of birefringence and extinction direction. In figure 8 the temperature dependence of  $\varphi$  and  $\Delta n$  in  $\text{Pb}(\text{Mg}_{1/3}\text{Nb}_{2/3})_{0.67}\text{Ti}_{0.33}\text{O}_3$  are shown. The temperature dependence of  $\Delta n$  is in a good agreement with the previously reported curves [29]. The phase transition from phase II into phase III occurs at about 378 K



**Figure 7.**  $\text{Pb}(\text{Mg}_{1/3}\text{Nb}_{2/3})_{0.67}\text{Ti}_{0.33}\text{O}_3$  crystal in two different orientations,  $6^\circ$  apart, between crossed polarizers at room temperature.

and the further phase transition into the cubic phase is observed at 428 K. In phase II  $\varphi$  deviates by a few degrees from  $45^\circ$  and does not show any noticeable temperature variations.

### 3.3. Phase III

It is generally believed that the macroscopic symmetry of PMN–PT with PT content exceeding 0.37 is tetragonal. However, there are some recent data that suggest the existence of another low-symmetry phase at around  $x = 0.4$ . As a result of optical study of the phase transition of phase II to the higher-temperature phase III [20–23] it has been shown that the optical extinction in phase III is not consistent with tetragonal symmetry. The change of slope of  $T_c$  [17] with  $x$  of about 0.47 also indicates that a new phase different from tetragonal may exist in the range  $x = 0.3$ –0.47. Finally, dielectric measurements show that there is a dielectric permittivity peak that has much higher values in this compositional range compared with crystals of other compositions.

The deviation of macroscopic symmetry of phase III from tetragonal is clearly seen in the Metripol images shown in figure 3. The extinction directions for  $x > 0.295$  and for temperatures higher than 390 K obviously deviate from the [100] direction and are inconsistent with tetragonal symmetry.

The temperature dependence of  $\varphi$  for  $\text{Pb}(\text{Mg}_{1/3}\text{Nb}_{2/3})_{0.67}\text{Ti}_{0.33}\text{O}_3$  in figure 8 shows a jump associated with the phase transition from phase II to phase III. In phase II  $\varphi$  is approximately  $45^\circ$ ; it then exhibits a jump down to about  $30^\circ$  at the transition to phase III. Within phase III  $\varphi$  shows a further gradual reduction up to the phase transition to the cubic phase at 420 K, which results in an abrupt disappearance of birefringence. These observations give support to the previous experimental evidence [20–23] of low-symmetry distortions in this phase.

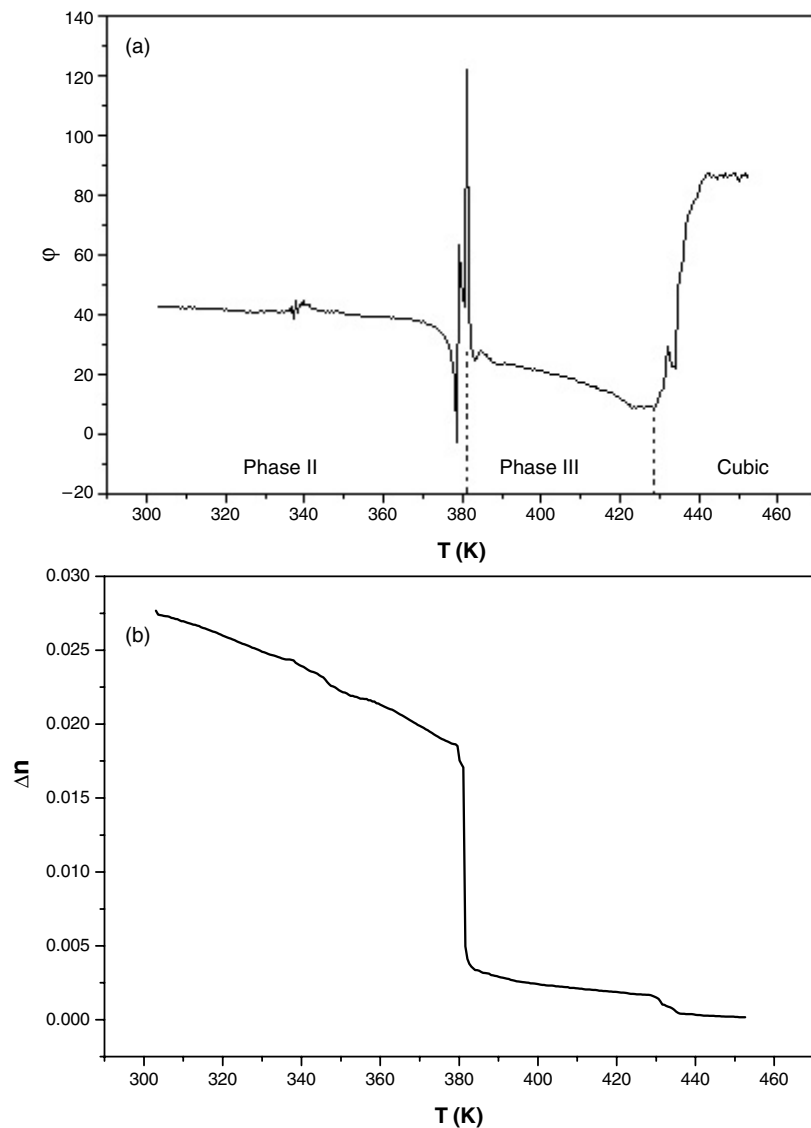


**Figure 8.** The temperature dependence of  $\varphi$  and  $\Delta n$  in  $\text{Pb}(\text{Mg}_{1/3}\text{Nb}_{2/3})_{0.67}\text{Ti}_{0.33}\text{O}_3$ . The rapid changes in  $\varphi$  seen near 380 K are an artifact caused by several changes in the period of  $|\sin \delta|$  at this temperature.

In figure 9 a  $\text{Pb}(\text{Mg}_{1/3}\text{Nb}_{2/3})_{0.62}\text{Ti}_{0.38}\text{O}_3$  crystal is shown as observed between crossed polars at two different orientations of the crystal. For  $T > 300$  K the crystal displayed only one phase transition from phase III to the cubic phase. Large and clear macrodomains were observed at room temperature. It can be seen that extinction is achieved in different domains at different angles. Some parts of the crystal do not show any extinction because of stacked twin domains. These observations clearly show that the macroscopic symmetry of phase III is not tetragonal, as has generally been believed hitherto, but must be of lower symmetry. Figure 10 shows the Metripol images of  $|\sin \delta|$  and  $\varphi$  for the same crystal. It can be seen that the birefringence is rather uniform and does not change significantly at the domain boundaries.

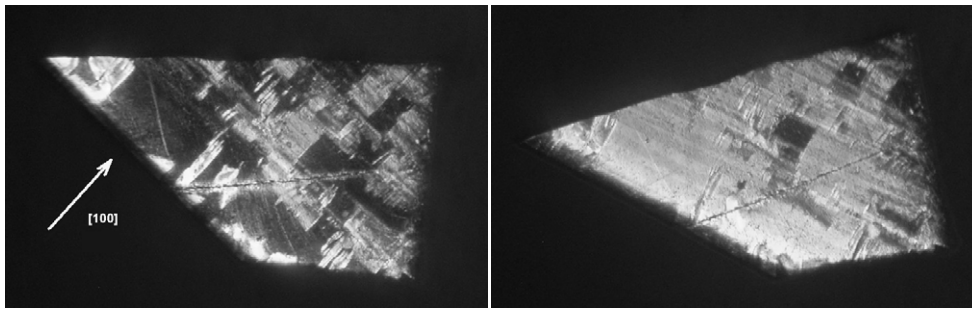


**Figure 9.**  $\text{Pb}(\text{Mg}_{1/3}\text{Nb}_{2/3})_{0.62}\text{Ti}_{0.38}\text{O}_3$  in two different orientations between crossed polars at room temperature. Extinction is achieved in different parts of the crystal at orientations  $15^\circ$  apart, indicating monoclinic symmetry.

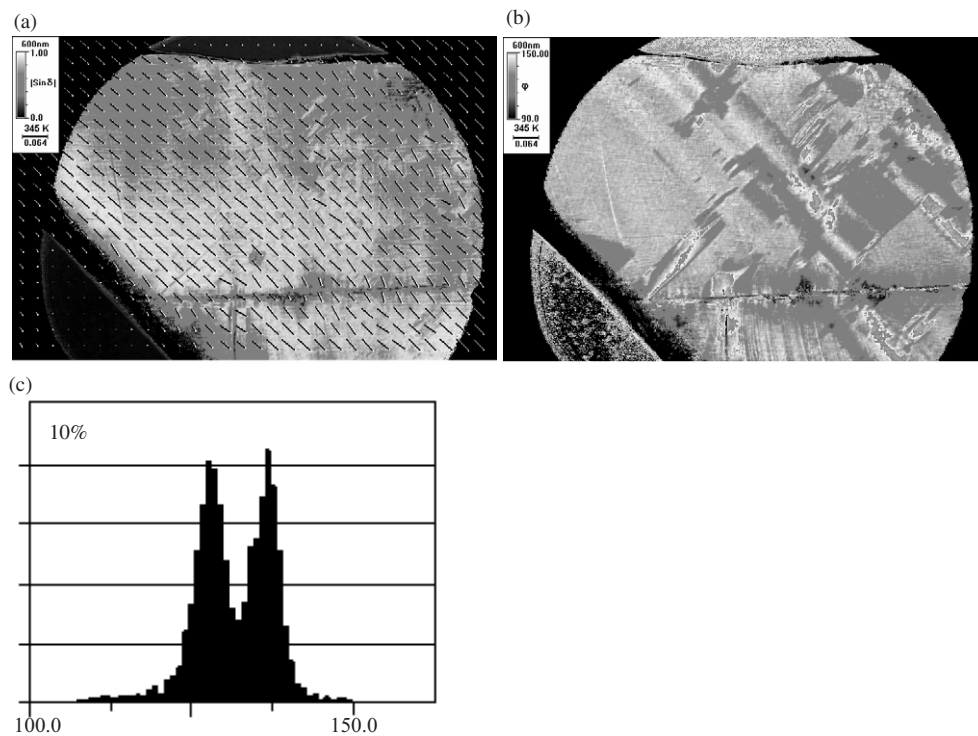


**Figure 10.** Metripol images of (a)  $|\sin \delta|$  and (b)  $\varphi$  for the crystal of  $\text{Pb}(\text{Mg}_{1/3}\text{Nb}_{2/3})_{0.62}\text{Ti}_{0.38}\text{O}_3$ . The horizontal scale bar is equal to 0.064 mm. (c) Histogram of the distribution of the angle  $\varphi$  taken over a region of the orientation image, with the two peaks approximately  $15^\circ$  apart.

The birefringence values in the two types of domains are almost equal and are much lower than those in phase II. They show the same temperature dependence (figure 11). However, contrast between the domains is clearly seen in the  $\varphi$  image, and the corresponding histogram of the distribution of the angle  $\varphi$  taken over a region of the orientation image shows the two peaks approximately  $15^\circ$  apart. We did not observe any noticeable temperature change of the domain structure in the crystal up to  $T_c$ . As can be seen from the Metripol image in one of the

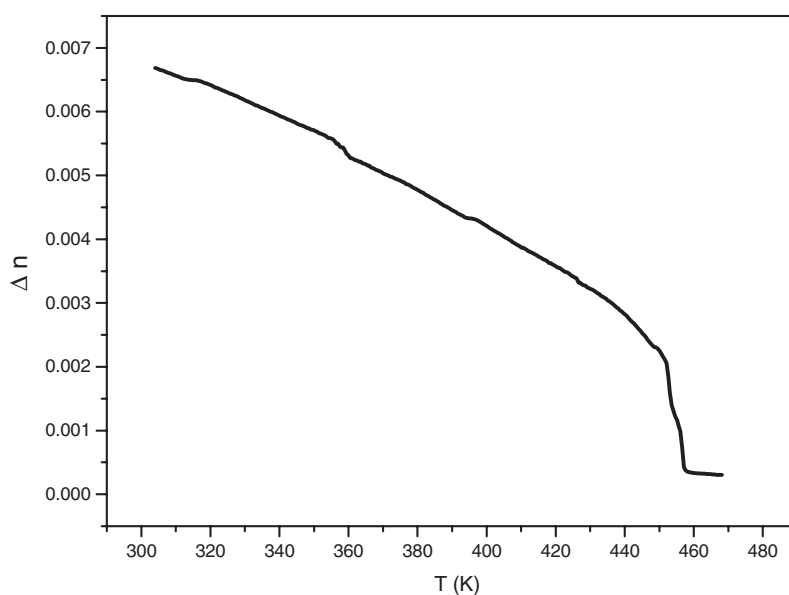


**Figure 11.** The temperature dependence of  $\Delta n$  in  $\text{Pb}(\text{Mg}_{1/3}\text{Nb}_{2/3})_{0.62}\text{Ti}_{0.38}\text{O}_3$ .

domains the marked extinction direction is parallel to [100], while in the other it was found to form an angle of  $16^\circ$  with this direction. These orientations are consistent with  $Pm$  symmetry.

We failed to find a clear boundary between the monoclinic phase III and the tetragonal phase T. Most of the crystals show a complicated domain structure, which makes it difficult to distinguish such a boundary. However, all the crystals with  $x < 0.47$  had parts that showed no extinction, while for those with  $x > 0.47$  the observations were consistent with tetragonal symmetry. This allows us to suggest that the boundary is located at about this value. Moreover, the change of slope for  $T_c$  as a function of  $x$  demonstrated in our previous paper [17] at about  $x = 0.47$  gives further support to this conclusion.

### 3.4. The phase diagram

In figure 12 the resulting phase diagram derived from all the observations is presented. This shows that for  $x = 0.3$ – $0.47$  there are two different low-symmetry phases. The extinction directions are consistent with  $Cm$  and  $Pm$  monoclinic symmetries. As has already been reported [17], the phase transition between these two monoclinic phases is of first order and shows a large thermal hysteresis. Thus the transformation from rhombohedral to tetragonal symmetry in PMN–PT occurs through two monoclinic phases.

The existence of these two monoclinic phases in PMN–PT has been proposed earlier from diffraction measurements [19]; however, the compositional ranges reported there are somewhat different from ours. Crystals with  $x < 0.3$  show a low birefringence and the extinction direction is consistent with rhombohedral symmetry, except for a narrow temperature range between 370 and 400 K. In this range in crystals with  $0.27 < x < 0.3$  the extinction angle rapidly approaches [100] and then hardly changes. Thus the possibility of tetragonal symmetry should be considered in this range, denoted in figure 12 as phase I'. This phase shows large hysteresis in  $T_c$  [17] and a domain structure which allows us to distinguish it from the monoclinic phase  $Pm$ (III) observed in crystals with  $x > 0.3$ .

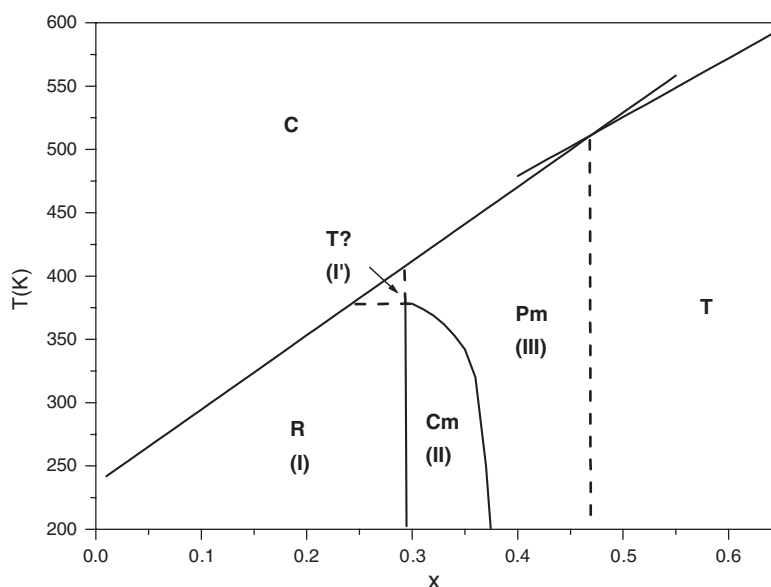


**Figure 12.** The refined phase diagram of PMN–PT, showing the symmetries of the different phases. The symmetry of phase I' is consistent with the tetragonal crystal system, but remains uncertain at the present time.

The advanced piezoelectric properties displayed for  $0.3 < x < 0.36$  [11, 30, 31] can be assigned to the  $Cm$  monoclinic phase. It is interesting to note that this phase also shows the highest birefringence compared with the phases either side [17]. On the other hand, the observed high dielectric permittivity peak [9, 10] is due to the phase transition from monoclinic  $Pm$  to the cubic phase.

### Acknowledgments

We are grateful to the Engineering and Physical Sciences Research Council (UK) for grants enabling this work to be carried out. We are also grateful to iBULe Photonics Co., Ltd (Korea) for the high-quality  $\text{Pb}(\text{Mg}_{1/3}\text{Nb}_{2/3})_{0.62}\text{Ti}_{0.38}\text{O}_3$  crystals kindly provided. We thank S Chowdhury for carrying out the electron microprobe analysis.

### References

- [1] Oguchi H, Nagano K and Hayakawa Sh 1965 *J. Am. Ceram. Soc.* **48** 630–5
- [2] Jaffe B, Cook W R and Jaffe H 1971 *Piezoelectric Ceramics* (London: Academic) p 136
- [3] Fu H and Cohen R E 2000 *Nature* **403** 281
- [4] Vanderbilt D and Cohen M H 2001 *Phys. Rev. B* **63** 094108
- [5] Glazer A M, Thomas P A, Baba-Kishi K Z, Pang G K H and Tai C W 2004 *Phys. Rev. B* **70** 184123
- [6] Kelly J, Leonard M, Tantigate C and Safari A 1997 *J. Am. Ceram. Soc.* **80** 957–64
- [7] Choi S W, Jung J M and Bhalla A S 1996 *Ferroelectrics* **189** 27–38
- [8] Noblanc O, Gaucher P and Calvarin G 1996 *J. Appl. Phys.* **79** 4291–7
- [9] Choi S W, Shrout T R, Jang S J and Bhalla A S 1989 *Ferroelectrics* **100** 29
- [10] Shrout T R, Chang Z P, Kim N and Markgraf S 1990 *Ferroelectr. Lett.* **12** 63–9
- [11] Service R E 1997 *Science* **275** 1878
- [12] Zhao X, Fang B, Cao H, Guo Y and Luo H 2002 *Mater. Sci. Eng. B* **96** 254–62

- [13] Ye Z-G, Noheda B, Dong M, Cox D and Shirane G 2001 *Phys. Rev. B* **64** 184114
- [14] Singh A K and Pandey D 2001 *J. Phys.: Condens. Matter* **13** L931–6
- [15] Noheda B, Cox D E, Shirane G, Gao J and Ye Z-G 2002 *Phys. Rev. B* **66** 054104
- [16] Xu G, Luo H, Xu H and Yin Z 2001 *Phys. Rev. B* **64** 020102
- [17] Zekria D, Shuvaeva V A and Glazer A M 2005 *J. Phys.: Condens. Matter* **17** 1593–600
- [18] Kiat J M, Uesu Y, Dkhil B, Matsuda M, Malibert C and Calvarin G 2002 *Phys. Rev. B* **65** 064106
- [19] Singh A K and Pandey D 2003 *Phys. Rev. B* **67** 064102
- [20] Tu C S, Hung L W, Chien R R and Schmidt V H 2004 *J. Appl. Phys.* **96** 4411–5
- [21] Tu C S, Tsai C L, Chen J S and Schmidt V H 2002 *Phys. Rev. B* **65** 104113
- [22] Tu C-S, Schmidt V H, Shih I-C and Chien R 2003 *Phys. Rev. B* **67** 020102
- [23] Zekria D and Glazer A M 2004 *J. Appl. Crystallogr.* **37** 143–9
- [24] Chien R, Schmidt V H, Tu C S and Hung L W 2004 *Ferroelectrics* **302** 581–5
- [25] Glazer A M, Lewis J G and Kaminsky W 1996 *Proc. R. Soc. A* **452** 2751–65 and [www.metripol.com](http://www.metripol.com)
- [26] Han J and Cao W 2003 *Phys. Rev. B* **68** 134102
- [27] Zhao X, Wang J, Chan H L W, Choy C L and Luo H 2003 *J. Phys.: Condens. Matter* **15** 6899–908
- [28] Bai F, Wang N, Li J, Viehland D P, Gehring M, Xu G and Shirane G 2004 *J. Appl. Phys.* **96** 1620–8
- [29] Ye Z-G and Dong M 2000 *J. Appl. Phys.* **87** 2312
- [30] Park S-E and Shrout T R 1997 *J. Appl. Phys.* **82** 1804
- [31] Kuwata J, Uchio K and Nomura S 1982 *Japan. J. Appl. Phys.* **21** 1298